Incorporation of chromium into hexagonal barium titanate: an electron paramagnetic resonance study

2005 J. Phys.: Condens. Matter 17 2763

(http://iopscience.iop.org/0953-8984/17/17/026)

INSTITUTE OF PHYSICS PUBLISHING JOURNAL OF PHYSICS: CONDENSED MATTER

J. Phys.: Condens. Matter **17** (2005) 2763–2774 doi:10.1088/0953-8984/17/17/026

Incorporation of chromium into hexagonal barium titanate: an electron paramagnetic resonance study

R Böttcher[1], E Erdem[1], H T Langhammer[2], T Müller[3] and H-P Abicht[3]

[1] Fakultät für Physik und Geowissenschaften, Universität Leipzig, Linnéstraße 5, 04103 Leipzig, Germany
[2] Fachbereich Physik, Martin-Luther-Universität Halle Wittenberg, Friedemann-Bach-Platz 6, 06108 Halle, Germany
[3] Fachbereich Chemie, Martin Luther-Universität Halle-Wittenberg, Kurt-Mothes-Straße2, 06120 Halle, Germany

Received 10 March 2005
Published 15 April 2005
Online at stacks.iop.org/JPhysCM/17/2763

Abstract

The EPR spectra of $BaTiO_3$ + 0.04 BaO + 0.01 Cr_2O_3 ceramics are studied in three frequency bands (9, 34 and 94 GHz). Three different, axially symmetric EPR spectra assigned to Cr^{3+} ions substituted at Ti sites corresponding to the different distorted octahedra in tetragonal and hexagonal crystal surroundings are observed at room temperature. The temperature dependence of the EPR spectra allowed the unambiguous assignment of the chromium ions to the lattice site in tetragonal and hexagonal modifications. The concentration measurements revealed that only 30% of the chromium is incorporated in the grains as Cr^{3+} ions whereas the remnant is in the EPR-silent tetravalent charge state or in Cr-rich secondary phases segregated at grain boundaries, pores and triple points. The intensity ratio of the two Cr^{3+} spectra in hexagonal $BaTiO_3$ depends on the preparation conditions.

1. Introduction

Barium titanate, $BaTiO_3$, represents a material system of fundamental importance for a wide range of technical applications. Although there have been, depending on temperature, different phases observed, the focus of research was on the cubic and tetragonal phases, which transform into each other at the paraelectric–ferroelectric phase transition temperature near 130 °C. Much less information is available about the hexagonal high temperature phase, which is stable at temperature > 1430 °C [1, 2].

The hexagonal polytype 6H-$BaTiO_3$ (h-$BaTiO_3$) crystallizes in the space group $P6_3/mmc$ with the lattice parameters $a = 0.5738$ nm and $c = 1.3965$ nm [3]. The unit cell is described by six BaO_3 layers (i.e. $[Ba(2)O(2)_3Ba(2)O(2)_3Ba(1)O(1)_3]_2$) forming a $(cch)_2$ sequence, where c corresponds to corner-sharing and h to face-sharing layers of the TiO_6 octahedra, respectively (for labelling the atoms see [1]). The atoms Ti(1) and Ti(2) occupy octahedra

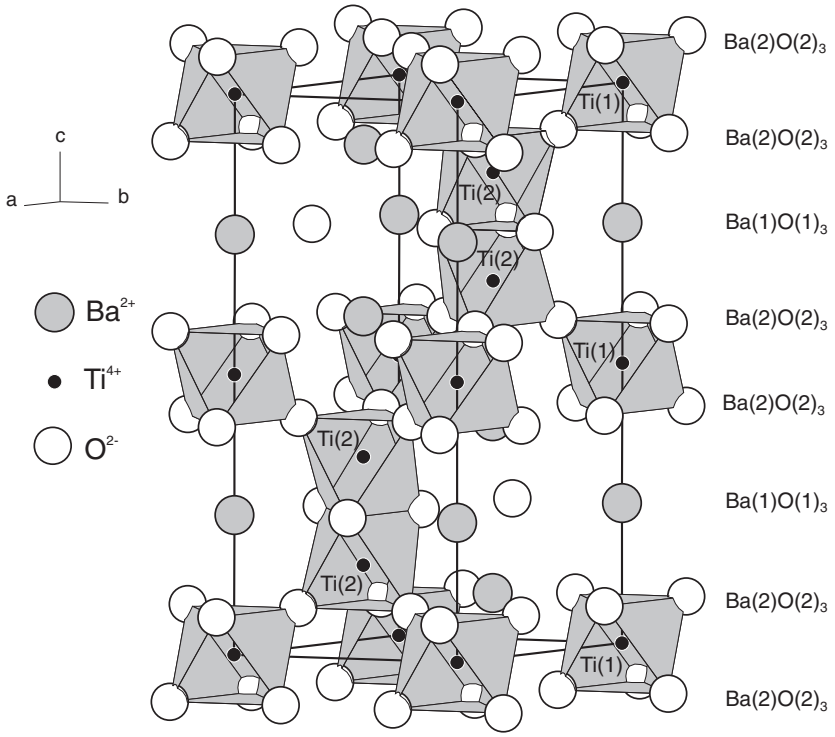

Figure 1. Schematic crystal structure of hexagonal (6H polytype) $BaTiO_3$.

which are exclusively corner connected and which share common faces, respectively, with rather short Ti(2)–Ti(2) distances in the Ti_2O_9 group of the face-sharing octahedra (figure 1). In contrast to the cubic crystal structure of $BaTiO_3$ the octahedra in h-$BaTiO_3$ are trigonally distorted in the *c* direction. The strength of trigonal distortion for the corner- and face-sharing octahedra is different. Therefore, in the hexagonal material there are two different Ti lattice sites. Four of the six Ti ions in the hexagonal unit cell are incorporated into the face-sharing octahedra whereas the other two are lying in the corner-sharing ones.

The stability range of the hexagonal phase can be extended to room temperature both by firing in reducing atmospheres (oxygen-deficient h-$BaTiO_3$) [4] and by doping with some acceptor-type 3d transition elements like Cr, Mn, Fe, Ni, or Cu [5–9] as well as with the elements Mg, Al, Ga, or In [10]. For undoped, oxygen deficient h-$BaTiO_3$ and Fe-doped h-$BaTiO_3$ it has been reported that oxygen is removed only from the oxygen sites O(1) sites in the $Ba(1)O(1)_3$ layers [11].

Hexagonal barium titanate undergoes successive phase transitions from the prototype phase (phase I) to phase II and phase III on cooling at 222 and 74 K, respectively. X-ray experiments with single-domain crystals revealed that phase II is orthorhombic with space group $C222_1$ [12]. Phase III is a ferroelectric phase and the crystal symmetry might be lower than the orthorhombic one [13]. In the low-temperature phase Noda *et al* performed high-resolution powder diffraction experiments and determined the lattice symmetry and unit cell parameters. As the space group of the ferroelectric phase they find the monoclinic group $P112_1$ [14, 15].

The aim of this paper is the investigation of the incorporation of chromium into hexagonal $BaTiO_3$. Because of the large difference of the effective ionic radii between Ba^{2+} (161 pm)

and Ti^{4+} (60.5 pm) [16] the incorporation of chromium ions with the tri- or tetravalent charge states onto the Ti sites in h-$BaTiO_3$ is very probable. The charge state of the ion determines its electron spin S unambiguously. Cr^{3+} is a $3d^3$ ion with $S = 3/2$ whereas the free ion Cr^{4+} has $S = 1$. Electron paramagnetic resonance (EPR) permits the determination of the charge state and the electronic ground state of the paramagnetic ion as well as its different incorporation sites in a solid. Through intensity measurements by means of EPR the occupancy fractions for Cr^{3+} ions at the Ti(1) and Ti(2) sites are estimated. To date no EPR investigations on chromium in h-$BaTiO_3$ are known in the literature whereas the Cr-EPR spectra of the other modifications are excessively analysed. Single-crystal studies were first reported by Müller *et al* [17]. From their temperature-dependent measurement the authors were able to demonstrate that the Cr^{3+} remains at the centre of the distorted oxygen octahedron in all ferroelectric phases. Possenriede *et al* [18] and Schwartz *et al* [19] pointed out that the Cr^{5+} ion ($3d^1$, $S = 1/2$) is only stable in the rhombohedral phase of $BaTiO_3$.

In this paper we present powder and single-crystal EPR spectra of chromium-doped h-$BaTiO_3$ measured in three different microwave-frequency bands, determine the spin-Hamiltonian parameters and discuss the incorporation of the Cr^{3+} ions and the charge compensation.

2. Experimental procedure

Ceramic samples with a nominal composition of $BaTiO_3$ + 0.04 BaO + 0.01 Cr_2O_3 were prepared by the conventional mixed-oxide powder technique. After mixing (agate balls, water) and calcining (1100 °C, 2 h) of $BaCO_3$ (Solvay, VL600, <0.1 mol% Sr) and TiO_2 (Merck, no 808), Cr_2O_3 (Merck, p.a.) was added to the $BaTiO_3$ powder. Then it was fine-milled (agate balls, 2-propanol) and densified to discs with a diameter of 12 mm and a height of nearly 3 mm. The samples were sintered in air at a temperature of 1400 °C for one hour. To avoid interfering contamination the samples were contained in ZrO_2 covered Al_2O_3 dishes.

The microstructure of polished and chemically etched specimens was examined by optical microscopy and by scanning electron microscopy (SEM). To determine the chromium distribution in the grains and intergranular regions, wavelength-dispersive x-ray electron probe microanalysis (WDX-EPMA) (model CAMEBAX, Camera, France) was performed. For the phase investigations at room temperature by XRD the sintered samples were crushed again and mixed with silicon powder for the purpose of calibration. The phase composition was determined quantitatively by analysing the intensity ratios $(111)_{\text{tetragonal}}/(103)_{\text{hexagonal}}$ and $(200)_{\text{tetragonal}}/(103)_{\text{hexagonal}}$ (D5000 diffractometer, Siemens, Germany). Before EPR measurements the ceramic discs were crushed in an alumina mortar. The spectra of non-crushed ceramic bodies are identical with ones of the powder samples but of lower overall signal strength. For the purpose of angular-dependent EPR measurements, single crystals with dimensions of about $0.3 \times 0.3 \times 0.2$ mm^3 were cut from ceramic samples with a main grain size of 500 μm. The nominal Cr content of these samples amounted to 5.0 mol%.

EPR measurements of pulverized samples were carried out in the X band (9 GHz) with a Varian E 112 spectrometer, in the Q band (34 GHz) with a Bruker EMX device and in the W band (94 GHz) with 100 kHz field modulation. The microwave frequencies were determined by electronic frequency counters and the magnetic field by means of a proton magnetic-resonance probe. The temperature dependence of the EPR spectra was taken using the Q band device with an Oxford cryostat CF 935 for the range from 4.2 to 300 K and the Varian E112 spectrometer with variable temperature accessory E 257. The single-crystal EPR measurements were performed on the Q-band spectrometer at room temperature rotating the single crystal in steps of 5° about an axis perpendicular to the hexagonal c-axis.

For the evaluation of the powder EPR spectra and the determination of the spin-Hamiltonian parameters the MATLAB[4] toolbox for electron paramagnetic resonance 'EasySpin 2.0.3' was used [20]. Simultaneously simulating the multi-frequency EPR spectra by variation of the input parameters, a high accuracy in the determination of the spectra parameters was achieved. For the quantitative analysis of the Cr^{3+} concentrations the double integrals of the simulated Q-band spectra were calculated. In order to determine the total Cr^3 concentration the sum of the double integrals of all partial spectra was compared with the double integral of our standard sample (blue ultramarine).

3. Results

For the discussion of the EPR findings it is important to recall that a powder spectrum is a superposition of spectra from randomly oriented crystallites. The resonance field $B_{\mathrm{res}}(\Omega)$, the intensity $A(\Omega)$ and the line width $\Gamma(\Omega)$ of a transition depend on the orientation Ω between the crystallite and the external magnetic field. The powder spectrum can be expressed as

$$P(B) = \int_{\Omega} A(\Omega) f(B - B_{\mathrm{res}}(\Omega), \Gamma(\Omega))\, \mathrm{d}\Omega \tag{1}$$

where $f(B - B_{\mathrm{res}}, \Gamma)$ is the line shape function and $\Omega = (\theta, \Phi)$, θ and Φ being the polar and azimuthal angles of the external magnetic field in the principal co-ordinate system of the spin Hamiltonian respectively [21, 22]. Replacing the line shape function by the Dirac delta function and transforming the natural co-ordinate, one obtains the stick spectrum as a line integral over the contour line $B_{\mathrm{res}} = B$

$$P(B) = \oint_{B_{\mathrm{res}}(\Omega)=B} \frac{A(\Omega)}{|\nabla B_{\mathrm{res}}(\Omega)|} \tag{2}$$

with

$$|\nabla B_{\mathrm{res}}| = \left[\left(\frac{\partial B_{\mathrm{res}}}{\partial \theta}\right)^2 + \frac{1}{\sin^2\theta}\left(\frac{\partial B_{\mathrm{res}}}{\partial \phi}\right)^2\right]^{1/2}. \tag{3}$$

It is evident from (3) that resonance lines are only observed when a change in the orientation of the external magnetic field B gives a very small change in the resonance field B_{res} (Ω). These orientations in which ∇B_{res} $(\Omega) = 0$ are termed polycrystalline critical points and give rise to singularities leading to either divergences or shoulders in the EPR powder pattern.

For the $^{50,52,54}Cr^{3+}$ ions with the electron $S = 3/2$ and the nuclear spin $I = 0$ we used the rhombic spin Hamiltonian of the form

$$\hat{H} = \beta \cdot \vec{B} \cdot \underline{\underline{g}} \cdot \vec{S} + D\left(\hat{S}_z^2 - \tfrac{1}{3}S(S+1)\right) + E\left(\hat{S}_x^2 - \hat{S}_y^2\right), \tag{4}$$

where g is the electronic g-tensor, β the Bohr magneton, and D and E the axial and rhombic fine structure (fs) parameters, respectively. In the case of the $^{53}Cr^{3+}$ ion (natural abundance 9.5%) with the nuclear spin $I = 3/2$ the spin Hamiltonian (4) must be augmented by the hyperfine (hf) term. Structural variations in the immediate surroundings of the chromium ions cause variations in the fs parameters. The fs parameter distributions are assumed to be random, so that they can be approximated by symmetric Gaussian distributions with the full width at half height ΔD and ΔE, respectively.

In the case of weak axial crystalline fields ($|D| \ll g\beta B$, $E = 0$) one gets three different types of polycrystalline critical points, $\theta_1 = 0$, $\theta_2 = \frac{\pi}{2}$, and $\theta_3 = 0.2322\pi$, and seven allowed transitions with the selection $\Delta M_{\mathrm{s}} = \pm 1$ (M_{s}, magnetic spin quantum number) are expected in

[4] MATLAB is a registered trademark of the MathWorks, Inc., Natick, MA, USA.

derivative powder spectrum as peaks or lines. The resonance field B_{res} of the central transition with $M_s = -\frac{1}{2} \leftrightarrow M_s = \frac{1}{2}$ has critical points for θ_1, θ_2, and θ_3. The intensities of the different fs transitions belonging to the orientation $\theta_1 = 0$ are very weak and their detection in the powder spectrum is hard. If the local symmetry of the Cr^{3+} is less than the axial one ($E \neq 0$) the peaks with $\theta_2 = \frac{\pi}{2}$ and $\theta_3 = 0.2322\pi$ are split by the orthorhombic fc parameter E.

In the case of strong axial crystalline field ($|D| \gg g\beta B$, $E = 0$) the fine-structure energy is the dominant term in the spin Hamiltonian. Under the assumptions $|D| \gg g\beta B$ and $E = 0$ the following expression is obtained for the effective g-factor g_{eff} of the Kramers doublet with $M_s = \pm\frac{1}{2}$ [23]:

$$g_{eff}(\theta) = \left[g_\parallel^2 + \left(4g_\perp^2 - g_\parallel^2\right)\sin^2\theta\right]^{\frac{1}{2}}\left[1 - \frac{3}{4}\frac{(g_\perp\beta B)^2}{(2D)^2}F(\theta)\right],$$

where

$$F(\theta) = \sin^2\theta\left[\frac{(4g_\perp + 2g_\parallel)\sin^2\theta - 2g_\parallel}{(4g_\perp - g_\parallel)\sin^2\theta + g_\perp}\right], \tag{5}$$

and $g_\parallel$ and $g_\perp$ are the principal values of the axial g tensor. The condition $|\nabla_\Omega B_{res}(\Omega)| = 0$ which reduces to $\left|\frac{\partial g_{eff}}{\partial\theta}\right| = 0$ results in the two polycrystalline critical points $\theta_1 = 0$ and $\theta_2 = \frac{\pi}{2}$. The effective g-values for the corresponding singularities are $g_{eff}(\theta_1) = g_\parallel$ and $g_{eff}(\theta_2) = 2g_\perp\left[1 - \frac{2(g_\perp\beta B)^2}{(2D)^2}\right]$, respectively. It should be emphasized that in this case also an orthorhombic distortion of crystalline field at the site of the paramagnetic ion generates an additional splitting of the line belonging to the point $\theta_2 = \frac{\pi}{2}$.

The first derivative of the absorption EPR spectrum of the Cr-doped $BaTiO_3$ powders measured in the X-band (9.1 GHz) at room temperature reveals an almost symmetrical line in the centre of the spectrum (figure 2) at $g \approx 1.97$ and five strong peaks lying outside the central part. Out of the scan range of this spectrum other very weak peaks were detected. In order to disentangle the X-band spectrum the frequency and the temperature dependences were investigated. In figure 3 the frequency dependence is depicted. Going from the X- to the W-band spectrum the number of the peaks is increased and distances between them in the central part of spectrum are decreased. The analysis permits the conclusion that the observed powder spectra can be divided into three partial spectra labelled by T1, H1 and H2, respectively (figure 2). They can be explained assuming the spin Hamiltonian (4) with the electron spin $S = 3/2$ and axial symmetry ($E = 0$) at room temperature. On this account, the observed spectra are assigned to Cr^{3+} ions at different lattice sites in hexagonal or tetragonal barium titanate. The overall XRD-measured phase composition of the ceramic samples investigated amounts to 11% tetragonal and 89% hexagonal phase.

The T1 spectrum, which is an overlay of peaks belonging to the transition $M_s = \frac{1}{2} \leftrightarrow M_s = -\frac{1}{2}$ and the orientations θ_1, θ_2, and θ_3, is attributed to Cr^{3+} at the Ti lattice site in tetragonal $BaTiO_3$. The peaks of the other fs transitions $M_s = \pm\frac{3}{2} \leftrightarrow M_s = \pm\frac{1}{2}$ are broadened and not detectable in the powder spectra of these samples. Only for this spectrum could the hyperfine transitions arising from $^{53}Cr^{3+}$ ($I = 3/2$) be resolved in the Q and W bands. The intensity of the T1 spectra correlates with the XRD results of the phase composition and the spin-Hamiltonian parameters are in agreement with the results of Müller *et al* [17] and Schwartz [19].

The H1 spectrum consists mainly of the peaks a and d (transition $M_s = \pm\frac{3}{2} \leftrightarrow M_s = \pm\frac{1}{2}$, orientation $\theta_1 = \frac{\pi}{2}$) as well as $b\left(\theta_2 = \frac{\pi}{2}\right)$ and $c(\theta_3 = 0.2322\pi)$. The latter two peaks pertain to the central transition $M_s = \frac{1}{2} \leftrightarrow M_s = -\frac{1}{2}$. The peak with $\theta_1 = 0$ and $M_s = \frac{1}{2} \leftrightarrow M_s = -\frac{1}{2}$ is overlapped by the strong T1 spectrum in the X-band spectrum and therefore not visible. Most important here, all the peak separations are determined by the fs parameters D and

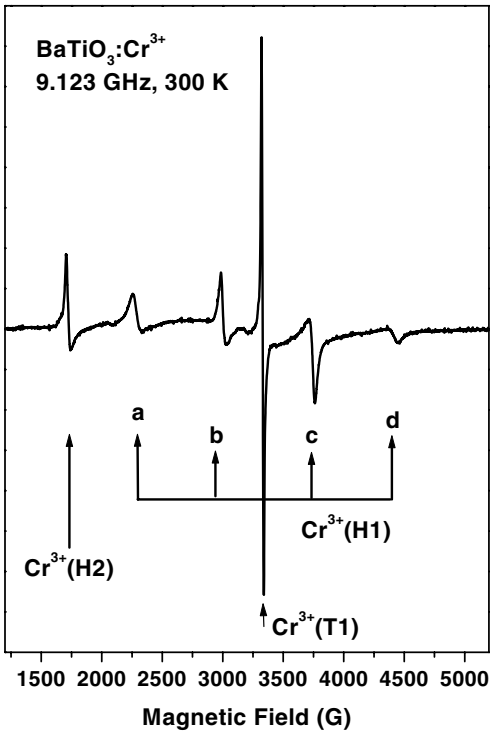

Figure 2. Room temperature EPR spectrum of the sample with a nominal composition of $BaTiO_3 + 0.04BaO + 0.01\ Cr_2O_3$, sintered at 1400 °C, measured in the X-band (9.1 GHz). Indicated are the corresponding peaks of the three different Cr^{3+} spectra.

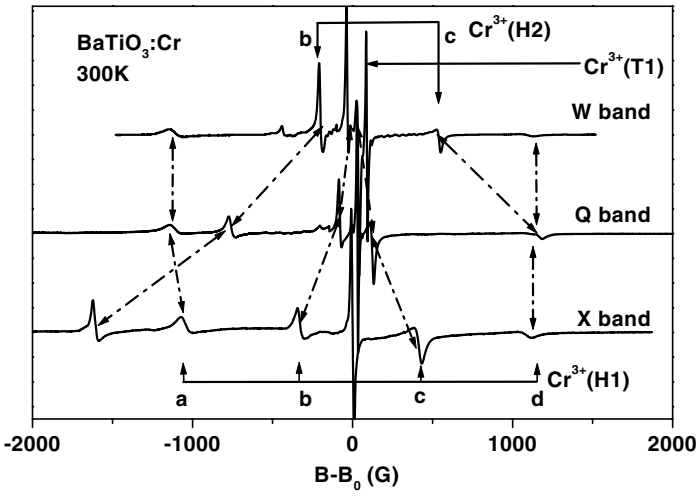

Figure 3. Room temperature EPR spectra of the same sample as in figure 2 measured in the X band (9.1 GHz), in the Q band (34.0 GHz) and in the W band (94.0 GHz) with $B_0 = \frac{h\nu}{g_\parallel \beta}$, $g_\parallel$ was taken from the H1 spectrum. Different transitions are marked by letters, related transitions by arrows. The transitions a and d of the spectrum Cr^{3+} (H2) are lying outside the scan range of the Q- and W-band spectrum.

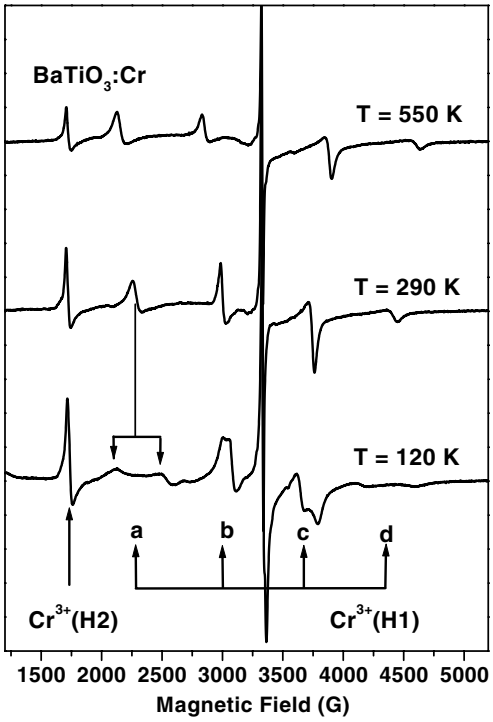

Figure 4. Temperature dependence of the X-band EPR spectra of the same sample as in figure 2. Below $T = 220$ K only the peaks of the H1 spectrum reveal splitting (marked only for peak a) due to symmetry reduction.

Table 1. Spin-Hamiltonian parameter of $Cr^{3+}_{Ti(1)}$ (H1) and $Cr^{3+}_{Ti(2)}$ (H2) impurities in 6H-$BaTiO_3$. The fs parameters and their dispersions and experimental errors are given in 10^{-4} cm^{-1}. The errors in the principal values of the g-tensors are ± 0.0006.

	T (K)	g_z	$g_{x,y}$	D	E	ΔD	ΔE
H1	300	1.9797	1.9857	1050(30)	—	70(5)	—
	170	1.9795	1.9860	980(30)	50(5)	70(5)	10(5)
	15	1.9795	1.9867	930(30)	80(5)	70(5)	10(5)
H2	300	1.9736	1.9756	3220(40)	—	120(10)	—
	170	1.9736	1.9756	3170(40)	—	120(10)	—
	15	1.9736	1.9756	3170(40)	—	120(10)	—

E (in the case of axial symmetry, proportional to $D^2/(g\beta B)$ and D for the b–c and a–d separations, respectively). The four peaks (a, b, c, d) were measured in all frequency (cf figure 3) bands so that the axial fs parameter D of this Cr^{3+} centre is much less than the Zeeman energy in the X band. The spin-Hamiltonian parameters given in table 1 were evaluated by simulating the multi-frequency spectra simultaneously using the function 'pepper' of the EasySpin toolbox [18]. The best adjustment was reached by using a dispersion ΔD of the fs parameter. The D-parameter reveals strong temperature dependence and decreases with falling temperature. Below $T = 220$ K the local symmetry of this Cr^{3+} centre is reduced from axial to orthorhombic symmetry, in agreement with the transmutation of the crystal structure of hexagonal barium titanate at the phase transition temperature $T_c = 222$ K (figure 4). In the ferroelectric phase of h-$BaTiO_3$ below 74 K the symmetry of this centre is also orthorhombic.

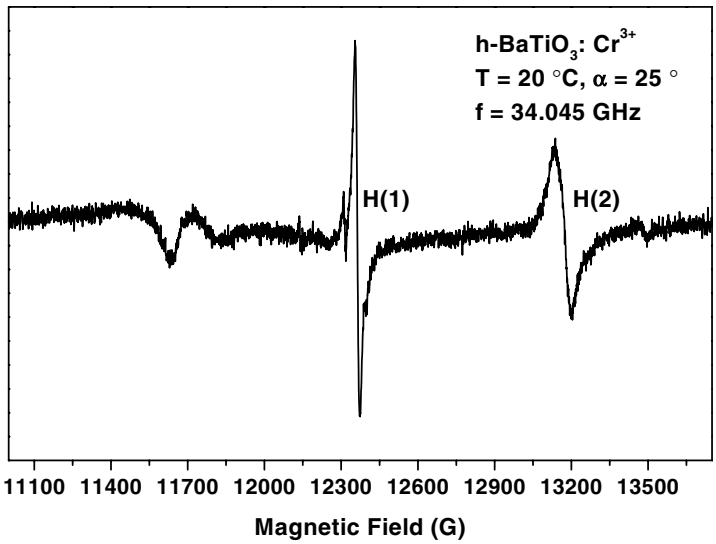

Figure 5. Single-crystal EPR spectrum of hexagonal $BaTiO_3$ doped with chromium. $T = 20\,^{\circ}C$, Q band ($f = 34.047$ GHz). The rotation axis is perpendicular to the hexagonal c-axis; the angle between the static magnetic field and the hexagonal axis is 25°. Only the central fine-structure lines of H1 and H2 centre are detected.

In contrast to the H1 partial spectrum the H2 X-band EPR spectrum only consists of one peak with $g_{\mathrm{eff}} = 3.79$. Going from the X to Q or W band more peaks belonging to this spectrum were detectable (figure 3), which can be classified in the same manner as in the case of the H1 spectrum. The analysis of the multi-frequency EPR spectra permits the conclusion that this axial Cr^{3+} EPR spectrum can be explained by an fs parameter D which is of the same order of magnitude as the X-band Zeeman energy. The spectral parameters in dependence on the temperature are also given in table 1. Note that its spin-Hamiltonian parameters are almost temperature independent. No additional splitting in this spectrum is observed below $T = 220$ K, although the H2 type is only found in $BaTiO_3$ samples with hexagonal fraction.

Figure 5 shows a single-crystal EPR spectrum of chromium-doped hexagonal $BaTiO_3$ measured in the Q band at room temperature. Due to the small size of our single crystals and the line broadening effects because of the dipole–dipole interaction caused by high concentration of the chromium ions only the central transition $M_s = 1/2 \leftrightarrow M_s = -1/2$ of the H1 and H2 spectrum was detected. The angular dependence for a rotation of the crystal about an axis perpendicular to the hexagonal c-axis is depicted in figure 6. Note that at room temperature the symmetry axis of the fine-structure tensor of the H1 and H2 centre is the hexagonal c-axis. The measured resonance of these two lines can be explained very well by the spin Hamiltonian (4) with the parameters given in table 1, which were derived from the EPR powder spectrum. The calculated resonance fields are represented by the drawn lines.

The Cr^{3+} concentration in the investigated powder samples determined by EPR intensity measurements amounts to about 30% of the nominal chromium concentration. Otherwise, the investigation of the Cr distribution inside the sintered samples by WDX-EPMA has shown that only 50–60% of the chromium is incorporated into the grown grains (main size about 100 μm). The remaining dopant forms Cr-rich secondary phases segregated at grain boundaries, pores and triple points. Hence, only about 50–60% of the Cr ions incorporated into the $BaTiO_3$ lattice are in the EPR-active Cr^{3+} state.

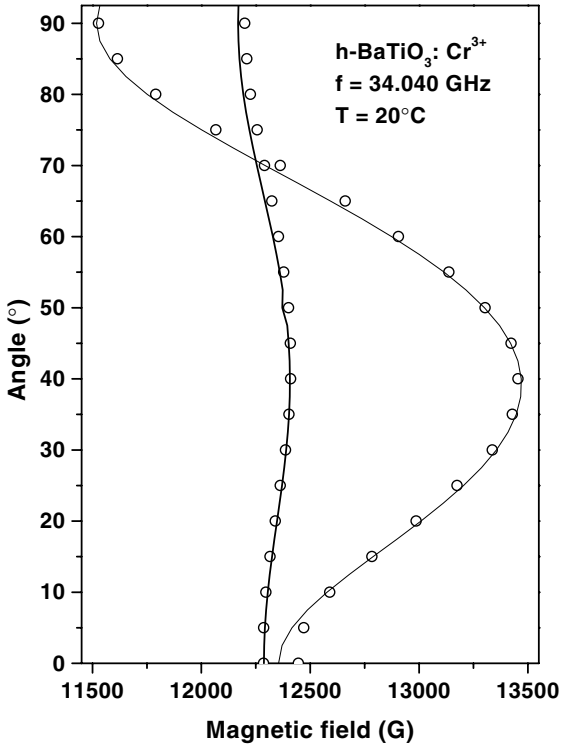

Figure 6. Angular dependence of the resonance fields of the central transition $M_s = 1/2 \leftrightarrow -1/2$ of the Cr^3 centres H1 and H2 in hexagonal $BaTiO_3$ (Q band). The rotation angle is the angle between the static magnetic field B and the hexagonal c-axis. $\alpha = 0°$ corresponds to $B \parallel c$.

The intensity ratio $I(\mathrm{H2})/I(\mathrm{H1})$ of the two spectra assigned to Cr^{3+} ions which are incorporated into the hexagonal $BaTiO_3$ is strongly dependent on the preparation conditions of the samples and varies from 2.2 to 1.7. The intensity of the T1 spectrum corresponds to the fraction of the tetragonal phase (11%) measured by XRD.

4. Discussion

The observed EPR spectra in our Cr-doped $BaTiO_3$ samples are assigned to Cr^{3+} ions incorporated into grains with 3C- or 6H-stacking order. Because of the large difference of the effective ionic radii [16] between Ba^{2+} (161 pm) and Ti^{4+} (60.5 pm) the incorporation of Cr^{3+} (60 pm) at Ti sites is probable. The experimentally determined electron spin of the paramagnetic ions ($S = 3/2$), the magnitude of the spin-Hamiltonian parameters, and the lack of any hyperfine structure in the X-band spectra give rise to this conclusion.

The T1 powder spectrum is explained by the same spin-Hamiltonian parameters as given by Müller [17] for Cr^{3+} ions substituted on Ti sites in $BaTiO_3$ single crystals. Also the same temperature dependences of the fine-structure parameters in the different phases are measured in the powder samples as known from single-crystal EPR investigations. Therefore, the T1 spectrum is caused by Cr^{3+} ions substituted at Ti lattices in the tetragonal modification of the $BaTiO_3$ ceramics. Its EPR intensity is a measure for the tetragonal fraction in the material. As the symmetry of the T1 spectrum is given by the local symmetry of the Ti lattice site, the

oxygen vacancy defect caused by the preservation of the electro-neutrality due to the charge misfit of the Cr^{3+} ions is not lying in its immediate surroundings. Each chromium ion is encircled by six oxygen ions.

The EPR spectra H1 and H2 are assigned to Cr^{3+} ions substituted at Ti^{4+} lattice sites of the hexagonal modification. Since in the hexagonal phase of $BaTiO_3$ two different Ti lattice sites Ti(1) and Ti(2) exist, the occurrence of two different Cr^{3+} EPR spectra with unequal spin-Hamiltonian parameters is expected. The H1 spectrum is assigned to Cr^{3+} ions on the Ti lattice site in the corner-sharing octahedra $Ti(1)O(2)_6^{8-}$ in which the Ti(1)–O(2) distances are equal. Due to the hexagonal crystal structure at room temperature the symmetry of this lattice site is reduced to the trigonal one by the presence of the next-nearest neighbours. Only a weak electric field arises, which is responsible for the smaller fine-structure parameter. Therefore, an EPR spectrum with axially symmetrical g and fine-structure tensor whose symmetry axes are parallel to the hexagonal c-axis is expected. This assumption is confirmed by single-crystal measurements. On the basis of the magnitude of the fine-structure parameter D and its strong temperature dependence one can conclude that also in this case the chromium ion does not generate an associate with an oxygen vacancy. Another argument for this statement is the fact that the symmetry of the EPR spectrum reflects the local symmetry of this Ti lattice site. Corresponding to the change of the hexagonal crystal symmetry to the orthorhombic one at the phase transition temperature $T_c = 222$ K, the symmetry of the spin Hamiltonian varies; below T_c an orthorhombic H1 spectrum is observed. The orthorhombic fine-structure parameter E is also a function of temperature.

The fits of the H1 spectrum measured at different temperatures could be improved by introducing a Gaussian distribution of the fs parameters with the width ΔD and ΔE. Because these parameters are very small in comparison with mean values D and E (table 1) there are only small structural variations in the immediate surroundings of the Cr^3 ion.

In contrast to the H1 spectrum, the other Cr^{3+}-EPR spectrum in the hexagonal $BaTiO_3$ modification, the H2 spectrum, reveals very weak temperature dependence. Its axial symmetry is stable from 10 to 500 K and no splitting of the peaks due to rhombic distortion could be detected in the full temperature range. We assign this H2 spectrum to Cr^{3+} ions substituted at one Ti lattice site in the Ti_2O_9 groups. In the face-sharing octahedra of a Ti_2O_9 group each Ti(2) is surrounded by three O(1) and O(2) oxygen. Due to the different Ti(2)–O(1) and Ti(2)–O(2) distances a strong electrical field arises at the Ti site and generated a larger fine structure splitting of the H2-centre. As a result of the temperature independence of the spin-Hamiltonian parameters one can speculate that associates between Cr^{3+} ions and oxygen vacancies, $Cr'_{Ti(2)}$–$V_O^{\bullet\bullet}$,[5] are formed. For this centre an axially symmetric spin Hamiltonian is expected and the symmetry axis of the g and fs tensors must be parallel to the connecting line $Cr'_{Ti(2)}$–$V_O^{\bullet\bullet}$ which is not lying in the hexagonal c-axis. The superposition model introduced by Newman and Urban [24] enables the determination of fs parameters for a model structure of a paramagnetic defect in a solid-state material. Using this model the estimated fs parameter D of the $Cr'_{Ti(2)} - V_O^{\bullet\bullet}$ centre is larger by a factor of five to eight (depending on the chromium–oxygen distance in the model) than the experimentally determined magnitude [25]. Therefore, we believe that the Cr^{3+} ions on Ti(2) lattice site are also isolated paramagnetic defects. In this defect model the symmetry axis of the g and fs tensor must be parallel to the hexagonal c-axis, as was proved by single-crystal EPR investigation. By the incorporation of Cr^{3+} ions at Ti(2) sites in face-sharing octahedra the trigonal symmetry of the Ti_2O_9 groups is locally stabilized in the full temperature range from 10 to 500 K. One reason for the symmetry stabilization is the shortening of the Cr^{3+}/Ti^{4+} metal–metal bond distance in these groups.

[5] Here the defect notation of Kröger/Vink is used.

In contrast to Mn^{4+}-doped h-$BaTiO_3$, in which the paramagnetic ion only substitutes at the Ti(1) site [26], in the case of chromium-doped hexagonal material both Ti(1) and Ti(2) sites are occupied by Cr^{3+} ions. By variation of the preparation conditions (sinter temperature and excess of BaO) the occupation probabilities of Cr^{3+} ions can be changed in a broad range. Crystal structure and related properties of chromium-doped barium titanate are discussed in detail in a further paper [27].

5. Conclusions

$BaTiO_3$ ceramics doped with 2 mol% chromium contain tetragonal and hexagonal phase parts of which the percentage strongly depends on impurities, stoichiometry and sintering conditions. At room temperature this material reveals three axially symmetric EPR spectra which are assigned to Cr^{3+} ions ($S = 3/2$). They are substituted at Ti^{4+} lattice sites in tetragonally and trigonally distorted octahedra, which reflect their tetragonal and hexagonal crystal surroundings. In contrast to manganese-doped hexagonal $BaTiO_3$ in which the Mn^{4+} ion ($S = 3/2$) only substitutes at the Ti(1) lattice site in the corner-sharing octahedra, both the Ti(1) and the Ti(2) (face-sharing octahedron) sites are occupied by Cr^{3+} ions. By variation of the preparation conditions (sinter temperature and excess of BaO) their occupation probabilities with Cr^{3+} can be changed in a broad range. Only 30% of the added chromium is incorporated in the grains as Cr^{3+} ions whereas the remnant is in the EPR-silent tetravalent charge state or in Cr-rich secondary phases segregated at grain boundaries, pores, and triple points.

Acknowledgments

The authors thank Mrs U Heinich and J Hoentsch (University Leipzig), C Teutloff (FU Berlin) for the measurements of the EPR spectra, and Professor Dr D Michel (University Leipzig) for helpful discussions. These investigations were financially supported by the Deutsche Forschungsgemeinschaft (SPP 'Hochfeld-EPR in Biology, Chemistry and Physics').

References

[1] Burbank R D and Evans H T Jr 1948 *Acta Crystallogr.* **1** 330
[2] Kirby K W and Wechsler B A 1991 *J. Am. Ceram. Soc.* **74** 1841
[3] Akimoto J, Gotoh Y and Oosawa Y 1994 *Acta Crystallogr.* C **50** 160
[4] Sinclair D C, Skakke J M S, Morrison F D, Smith R I and Beales T P 1999 *J. Mater. Chem.* **9** 1327
[5] Glaister R M and Kay H F 1960 *Proc. Phys. Soc.* **76** 763
[6] Ren F, Ishida S and Mineta S 1994 *J. Ceram. Soc. Japan* **102** 3026
[7] Dickson J G, Katz L and Ward R 1961 *J. Am. Chem. Soc.* **83** 3026
[8] Langhammer H L, Müller T, Felgner K-H and Abicht H-P 2000 *J. Am. Ceram. Soc.* **83** 605
[9] Langhammer H L, Müller T, Böttcher R and Abicht H-P 2003 *Solid State Sci.* **5** 965
[10] Keith G M, Rampling M J, Sarma K, Mc Alford N and Sinclair D C 2004 *J. Euro. Ceram. Soc.* **24** 1721
[11] Grey J E, Li Ch, Cranswick L M D, Roth R S and Vanderah T A 1998 *J. Solid State Chem.* **135** 312
[12] Sawaguchi E, Akishige Y and Kobayashi M 1985 *J. Phys. Soc. Japan* **54** 480
[13] Yannaguchi H, Uwe H, Sakudo T and Sawaguchi E 1988 *J. Phys. Soc. Japan* **57** 147
[14] Noda Y, Akiyama K, Shobu T, Kuroiwa Y and Yamaguchi H 1999 *Japan. J. Appl. Phys. Suppl.* **38** 73
[15] Noda Y, Akiyama K, Shobu T, Kuroiwa Y, Nakao H, Mori Y and Yamaguchi H 1998 *Ferroelectrics* **217** 1
[16] Shannon R D 1976 *Acta Crystallogr.* A **32** 751
[17] Müller K A, Berlinger W and Albers J 1985 *Phys. Rev.* B **32** 5837
[18] Possenriede E, Schirmer O F, Albers J and Godefroy G 1990 *Ferroelectrics* **107** 313
[19] Schwartz R N and Wechsler B A 1993 *Phys. Rev.* B **48** 7057
[20] Stoll St 2003 Spectral simulations in solid-state EPR *PhD Thesis* ETH Zurich

[21] Weil J A, Wertz J E and Bolton J R 1994 *Electron Spin Resonance: Elementary Theory and Practical Applications* (New York: Wiley)
[22] Kliava J 1986 *Phys. Status Solidi* b **134** 441
[23] Kirkpatrick E S, Müller K A and Rubins R S 1964 *Phys. Rev.* **135** 86A
[24] Newman D J and Urban W 1975 *Adv. Phys.* **24** 24
[25] Müller K A 1986 *J. Phys. Soc. Japan* **55** 719
[26] Böttcher R, Langhammer H T, Müller T and Abicht H-P 2005 at press
[27] Langhammer T H, Müller T, Böttcher R and Abicht H-P 2005 at press